CSIRO PUBLISHING

International Journal of Wildland Fire
http://dx.doi.org/10.1071/WF13157

Calibration of the Fire Weather Index over Mediterranean Europe based on fire activity retrieved from MSG satellite imagery

Carlos C. DaCamara[A,E], *Teresa J. Calado*[A], *Sofia L. Ermida*[A], *Isabel F. Trigo*[A,C], *Malik Amraoui*[A,B] and *Kamil F. Turkman*[D]

[A]Instituto Dom Luiz (IDL), Faculdade de Ciências, Universidade de Lisboa, Campo Grande, Edifício C8, Piso 3, PT-1749-016 Lisboa, Portugal.
[B]Universidade de Trás-os-Montes e Alto Douro (UTAD), Escola de Ciências e Tecnologia, Quinta de Prados, PT-5001-801 Vila Real, Portugal.
[C]Instituto Português do Mar e da Atmosfera (IPMA), Rua C do Aeroporto, Piso 3, PT-1749-077 Lisboa, Portugal.
[D]Departamento de Estatística e Investigação Operacional (DEIO), Centro de Estatística e Aplicações da Universidade de Lisboa (CEAUL), Faculdade de Ciências, Universidade de Lisboa, Campo Grande, Edifício C6, Piso 4, PT-1749-016 Lisboa, Portugal.
[E]Corresponding author. Email: cdcamara@fc.ul.pt

Abstract. Here we present a procedure that allows the operational generation of daily maps of fire danger over Mediterranean Europe. These are based on integrated use of vegetation cover maps, weather data and fire activity as detected by remote sensing from space. The study covers the period of July–August 2007 to 2009. It is demonstrated that statistical models based on two-parameter generalised Pareto (GP) distributions adequately fit the observed samples of fire duration and that these models are significantly improved when the Fire Weather Index (FWI), which rates fire danger, is integrated as a covariate of scale parameters of GP distributions. Probabilities of fire duration exceeding specified thresholds are then used to calibrate FWI leading to the definition of five classes of fire danger. Fire duration is estimated on the basis of 15-min data provided by Meteosat Second Generation (MSG) satellites and corresponds to the total number of hours in which fire activity is detected in a single MSG pixel during one day. Considering all observed fire events with duration above 1 h, the relative number of events steeply increases with classes of increasing fire danger and no fire activity was recorded in the class of low danger. Defined classes of fire danger provide useful information for wildfire management and are based on the Fire Risk Mapping product that is being disseminated on a daily basis by the EUMETSAT Satellite Application Facility on Land Surface Analysis.

Additional keywords: fire danger, fire management, generalised Pareto distribution, remote sensing, weather.

Received 10 June 2012, accepted 23 April 2014, published online 8 August 2014

Introduction

Representing more than 85% of burned area in Europe, the Mediterranean is one of the regions of the world most affected by large wildfires, which burn half a million ha of vegetation cover every year, causing extensive economic losses and ecological damage (San-Miguel-Ayanz *et al.* 2013).

Fire in the Mediterranean is a natural phenomenon (Mataix-Solera *et al.* 2011) linking climate, humans and vegetation (Lavorel *et al.* 2007). Fire activity is therefore conditioned by natural and anthropogenic factors. Natural factors include topography, vegetation cover and prevailing weather conditions (San-Miguel-Ayanz *et al.* 2003), which are linked to several atmospheric mechanisms working at different temporal and spatial scales (Trigo *et al.* 2006). At the regional and at the seasonal or inter-annual time scales, rainy and mild winters followed by warm and dry summers lead to high levels of vegetation stress that make the region particularly prone to the occurrence of fire events (Pereira *et al.* 2005). At the local and daily scales, extreme weather conditions (e.g. temperature, wind speed, atmospheric stability, fuel moisture and relative humidity) in turn play a key role in the ignition and spread of wildfires (Amraoui *et al.* 2013).

Land management practices and arson are crucial anthropogenic factors in Mediterranean Europe, being responsible for ~90% of fire ignitions (Moreno *et al.* 1998). Depopulation of rural areas and associated conversion of agricultural fields into forest plantations, shrublands or woodlands are also major anthropogenic factors that contribute to increased fuel availability (Pausas and Vallejo 1999; Lloret *et al.* 2002). Anthropogenic factors further include fire management policies that comprise fire prevention, fire pre-suppression and fire suppression measures (Fernandes 2008). Since 1990 the European Commission has been implementing actions aiming at the organisation of a community forest fire information system and at the development and implementation of advanced methods for the evaluation of forest fire danger and the estimation of burned areas at the European scale. An outcome of these actions is the so-called Fire Danger Forecast module of the European Forest Fire Information System (EFFIS), which may be taken as a reference at the European level (San-Miguel-Ayanz *et al.* 2012). The module is currently generating daily maps of 1–6 days projected fire danger level in the European Union at two different spatial scales based on weather forecast data at 10-km resolution from Météo-France and at 25-km resolution from the Deutsche Wetter Dienst (DWD), which are the respective French and German weather services.

Forecasts of fire danger over Mediterranean Europe up to 3 days in advance are also currently being disseminated within the framework of the Satellite Application Facility on Land Surface Analysis (LSA SAF, Trigo *et al.* 2011), which is part of the distributed Applications Ground Segment of EUMETSAT (the European Organization for the Exploitation of Meteorological Satellites). The aim of the LSA SAF is to generate and disseminate a suite of products to support land, land–atmosphere and biosphere applications, taking full advantage of remotely sensed data provided by EUMETSAT's two main satellite systems: the geostationary series, Meteosat Second Generation (MSG), and the EUMETSAT Polar System (EPS).

The University of Lisbon has been coordinating the Fire Detection and Monitoring (FD&M) and the Fire Risk Mapping (FRM) products that integrate the subset of LSA SAF products related to wildfire applications (Trigo *et al.* 2011). The FD&M product takes advantage of the high temporal resolution of SEVIRI, the radiometer on-board MSG satellites, to detect and monitor active fires every 15 min over Africa and Europe (Amraoui *et al.* 2010). The FRM product currently consists of forecasts of fire danger over Mediterranean Europe based on a statistical procedure that incorporates FD&M-derived information about active fire history, together with daily meteorological data provided by the European Centre for Medium-Range Weather Forecasts (ECMWF). Meteorological information is used to derive the so-called Fire Weather Index (FWI) that has proven to be especially adequate to rate fire danger over the Mediterranean (Viegas *et al.* 1999).

The goal of the present study is to quantify and predict the randomness in the distribution of duration of fire events using statistical modelling, and therefore provide a robust estimation of fire danger instead of a simple characterisation using basic FWI statistics. First, it is demonstrated that statistical models based on two-parameter generalised Pareto (GP) distributions adequately fit the observed samples of fire duration and that these models are significantly improved when FWI is integrated as a covariate of scale parameters of the GP distributions. Fire duration corresponds to the total number of hours in which fire activity is detected in the same pixel during a single day. Probabilities of fire duration exceeding specified thresholds allow estimation of meteorological fire danger, which is then used to calibrate FWI, leading to the definition of five classes of fire danger. Performance of the obtained classification is finally assessed by analysing the distribution of fire duration among classes of fire danger. Defined classes provide useful information for wildfire management and are based on daily maps of fire danger operationally generated over Mediterranean Europe by the LSA SAF.

Background

Fire prevention requires adequate knowledge about when and where a fire event is likely to occur, and the potential damage that may result to wildland and urban values (Finney 2005). These two aspects, respectively referred to as fire danger and vulnerability, constitute the two main components of fire risk assessment (Chuvieco *et al.* 2010). The first component deals with fire behaviour probabilities and wildfire potential assessment that encompasses potential fire ignition, propagation and difficulty of control. The vulnerability component includes the assessment of the negative effects, which mainly relate to socioeconomic values, and degradation potential of soil, vegetation conditions and landscape value.

The focus of the present study is on wildfire potential assessment that is usually based on fire danger rating systems (Fujioka *et al.* 2008), which provide indices to be used on an operational basis for fire prevention management. Because of the availability of near-real time weather observations and forecasts, most danger rating systems make use of indices based on meteorological parameters (Bovio and Camia 1997).

Here, fire danger is rated based on the FWI component of the Canadian Forest Fire Weather Index System (CFFWIS, Van Wagner 1974; Stocks *et al.* 1989). CFFWIS has proved to be particularly suitable as a fire rating system for Mediterranean Europe. Viegas *et al.* (1992), Chuvieco *et al.* (2009) and Dimitrakopoulos *et al.* (2010) uncovered relationships between fuel moisture content and fire occurrences in forested areas and shrublands of Portugal, Spain and Greece. Carvalho *et al.* (2008) showed that more than 80% of the variability in monthly burned area in Portugal can be explained by means of components of CFFWIS. Similar results were obtained by Camia and Amatulli (2009) for Mediterranean Europe. Pereira *et al.* (2013) developed a multiple linear regression model that is able to explain 63% of the total observed variance of the decimal logarithm of the monthly burned areas in July and August for 1980–2011. As independent variables, the model uses the Daily Severity Rating (an index derived from FWI) in the pre-fire season (May and June) and in the fire season (July and August). Viegas *et al.* (1999) analysed the performance of six different methods of fire rating and found that FWI presented the best results, both with respect to the number of fires and to the burned area per day. Dimitrakopoulos *et al.* (2011) showed that CFFWIS components, in particular FWI, are suitable to rate fire danger in the eastern Mediterranean. Since 2007, FWI has been the main component of the EFFIS Danger Forecast module (San-Miguel-Ayanz *et al.* 2012).

When applied to ecosystems other than Canadian forests, CFFWIS must be calibrated to the new environmental conditions by means of a reliable database of fire events (Viegas *et al.* 2004; Carvalho *et al.* 2008). The process of calibration usually involves establishing a set of break points that result from the analyses of fire weather history and time series of the CCFFWIS components, namely FWI (Van Wagner 1987). Established break points are then used to define fire danger classes (Kiil *et al.* 1977). Classification of FWI values into fire danger classes may be performed by means of logistic regression (Andrews *et al.* 2003; Dimitrakopoulos *et al.* 2011; Šturm *et al.* 2012) or by setting up the lower limit of the upper class and then estimating the remaining thresholds based on a geometric progression (Van Wagner 1987). The latter approach was adopted by EFFIS where the lower limit of the upper class is estimated from a large sample of FWI values associated with large fire events of more than 500 ha of burned area (San-Miguel-Ayanz *et al.* 2012). Amraoui *et al.* (2013) suggest using spatial and temporal information on fire activity at the pixel level to statistically calibrate weather-based indices of fire danger associated with a given class of vegetation. This approach is followed in the present study where breakpoints of FWI are based on estimates of fire danger provided by statistical models of fire activity based on the FD&M product from the LSA SAF. The proposed approach has the advantage of rating fire danger based on statistical models of extreme fire events, which allow quantifying the contribution of meteorological factors in terms of increasing or decreasing the probability that the duration of a fire event exceeds a given threshold.

Data and methods

Study area

Encompassing Mediterranean Europe, the study area (Fig. 1) is delimited by the latitude circles of 35 and 45°N and the meridians of 10°W and 37°E. In order to be consistent with related LSA SAF products, all data fields are mapped in the so-called Normalised Geostationary Projection (NGP) of MSG (EUMETSAT 1999), which represents an idealised earth as seen from a virtual MSG satellite located over the equator at the nominal longitude of 0° and at a distance of 42 164 km from the centre of the earth. Because the image acquisition process by MSG is based on constant angular steps seen from the geostationary orbit, the MSG pixel resolution of 3 km at the nominal sub-satellite point (0° latitude, 0° longitude) progressively deteriorates with increasing distance, reaching values of ~5 km over Mediterranean Europe (EUMETSAT 2010).

Baseline information about land cover is obtained from the 1-km resolution Global Land Cover 2000 (GLC2000) dataset as derived from SPOT-4 VEGETATION (Bartholomé and Belward 2005). GLC2000 data comprise 22 land-use types grouped into three main classes of vegetation cover (Fig. 1): forests (GLC2000 classes 1, 2, 4 and 6), shrublands (classes 11, 12 and 14) and cultivated areas (class 16). The three main classes were mapped from the original 1-km resolution to the NGP of MSG by assigning to each (~5-km) MSG pixel the most frequent class falling inside that pixel.

Study period

The study covers the months of July and August of 2007, 2008 and 2009. This period may be regarded as representative of fire activity in Mediterranean Europe taking into account the annual amounts of burned area for Portugal, Spain, France, Italy and Greece (European Commission 2008, 2009, 2010, 2011).

A summary of the official statistics in those five Southern Member States of the European Union is provided in Table 1. During 2007, the total burned area is well above the average that was recorded during the period 1980–2010. There is also a very high contrast between western and eastern Mediterranean Europe, with Italy and Greece contributing to 80% of the total

Table 1. Burned area in five states of Mediterranean Europe

The first pair of rows presents the average burned area for the period 1980 to 2010 in Portugal, Spain, France, Italy and Greece. The following three pairs of rows present the burnt areas in the five countries for 2007, 2008 and 2009. Data were provided by European Commission (2011)

Burned areas (ha)	Portugal	Spain	France	Italy	Greece	Total
1980–2010	109 386	173 169	27 504	114 276	47 309	471 644
%	23	37	6	24	10	100
2007	31 450	82 048	8 570	227 729	225 734	575 531
%	5	14	2	40	39	100
2008	17 244	39 895	6 001	66 329	29 152	158 621
%	11	25	4	42	18	100
2009	87 416	110 783	17 000	73 355	35 342	323 896
%	27	34	5	23	11	100

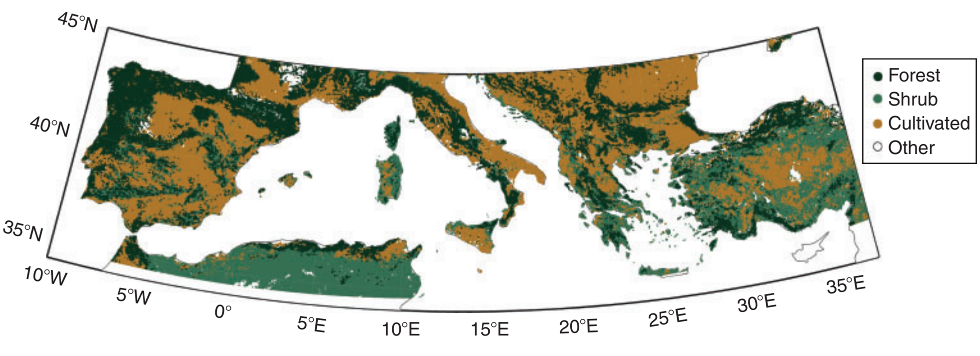

Fig. 1. Geographical distribution of the three main vegetation types as derived from GLC2000.

burned area; year 2007 was one of the worst fire years ever recorded in Italy, and the worst ever recorded in Greece (San-Miguel-Ayanz *et al.* 2013). Year 2008 saw very low fire incidence, the total area burned representing the minimum since the beginning of records in 1980. Year 2009 was also below the 1980–2010 average but nevertheless experienced double the burned area of 2008. When compared with 2007, 2009 shows the opposite – albeit less extreme – pattern for western and eastern Mediterranean Europe. In the case of Portugal, the burned area in 2009 was five times larger than in the previous year.

Meteorological data

Daily values of FWI over the study area are derived from meteorological fields provided by the ECMWF operational model for 12 UTC, for July and August from 2007 to 2009. Originally obtained over a $0.25 \times 0.25°$-latitude–longitude grid, the meteorological fields were re-projected onto NGP. Data consist of 2-m air temperature, 2-m dew point temperature, 10-m wind speed and 24-h cumulated precipitation. Temperature and dew point were topographically corrected by applying a constant lapse rate of $-0.67°\mathrm{C}\ 100\,\mathrm{m}^{-1}$ to the difference between ECMWF (coarser) orography and NGP pixel altitude. Relative humidity of air was computed by combining dew point temperature and temperature according to Magnus' expression (Lawrence 2005). For each pixel and day, anomalies of FWI, hereafter referred to as FWI^*, were computed as departures from the 30-year means for the reference period 1980–2009, that is, the anomaly FWI^*_{pd} for MSG pixel p and day d is defined as:

$$FWI^*_{pd} = FWI_{pd} - \overline{FWI}_p \tag{1}$$

where FWI_{pd} is the value of FWI for pixel p and day d and $\overline{FWI}_p$ is the time mean performed for that pixel and day over the 30-year reference period.

Fire activity and duration

Information on fire activity every 15 min on an MSG pixel basis is available from the abovementioned FD&M product that is currently generated within the framework of the LSA SAF (Trigo *et al.* 2011).

Let p be a given MSG pixel in the study area and let d be a given day during the study period. For each pixel p, at day d, there are 96 observations (one every 15 min) made by the SEVIRI instrument on-board MSG. Let $\mathbf{I}_{pd}(i)$ be an indicator function that is equal to 1 if the ith MSG image has captured fire activity inside pixel p during day d, and is equal to 0 otherwise. The indicator function may be used to reorganise information about fire activity on a daily basis in terms of fire duration δ_{pd}, which, for pixel p during day d, is defined as:

$$\delta_{pd} = 0.25 \times \sum_{i=1}^{96} \mathbf{I}_{pd}(i) \tag{2}$$

Units of δ are hours, the coefficient 0.25 converting into hours the sampling interval of 15 min between consecutive MSG images. Duration δ may vary from 0 (no fire activity detected at the considered pixel during the considered day) theoretically up to 24 h (fire activity detected in all 96 MSG images covering that day). Fire duration δ may be viewed as a proxy of fire intensity and burn extent but it should be noted that δ is not to be interpreted as the duration of individual fire events. This is because SEVIRI is capable of detecting fire activity in a given pixel of a given image, but is unable to identify different individual fire events inside a pixel and in contiguous pixels, either in space and time.

Statistical models of fire duration

The statistical distribution of fire duration δ is modelled using the 'peaks over threshold' (POT) approach (Pickands 1975), which is a commonly used tool to quantify fire danger (de Zea Bermudez *et al.* 2009; Mendes *et al.* 2010; Sun and Tolver 2012). The POT approach uses the GP distribution as a model to assign probabilities to the exceedances of duration δ over a threshold, that is, to values $x = \delta - \delta_{\min}$ (with $\delta > \delta_{\min}$) where $\delta_{\min}$ is a prescribed minimum value (de Zea Bermudez and Kotz 2010b). The POT approach is discussed in detail in Embrechts *et al.* (1997) and a thorough review of the application of the procedure to the analysis of large wildfires is provided in Holmes *et al.* (2008).

The GP probability density function g is given by:

$$g(x|\alpha,\sigma) = \frac{1}{\sigma}\left(1 + \frac{\alpha}{\sigma}x\right)^{-1-\frac{1}{\alpha}} \tag{3}$$

where x is the exceedance, and α and σ are the shape and scale parameters. The corresponding GP cumulative distribution function is:

$$G(x|\alpha,\sigma) = 1 - \left(1 + \frac{\alpha}{\sigma}x\right)^{-\frac{1}{\alpha}} \tag{4}$$

When $\alpha < 0$ the distribution is upper bounded, with $0 < x < -\sigma/\alpha$. A complete description of the GP distribution may be found in de Zea Bermudez and Kotz (2010a).

The minimum threshold $\delta_{\min}$ is estimated using a graphical approach (Coles 2001) where the chosen value is such that the sample mean of the values exceeding successive thresholds larger than $\delta_{\min}$ becomes a linear function when plotted against the respective thresholds. GP distributions also have the property of being stable with respect to excesses over threshold operations, that is, if x is a GP distribution with parameters (α, σ), then for any u, $x - u$ (with $x > u$) is also a GP distribution with parameters $(\alpha, \sigma - \alpha u)$ (Castillo and Hadi 1997). Choice of $\delta_{\min}$ is therefore confirmed by inspecting plots of α *v.* x and checking if $\delta_{\min}$ lies in the section of the curve where values of the shape parameters tend to stabilise after a steep decreasing. Choice of the minimum threshold is also conditioned by the need to have a sufficiently high value of $\delta_{\min}$ to ensure a weak temporal and spatial dependence of exceedances. As pointed out by Mendes *et al.* (2010), the POT method is carried under the assumption that the data are independent and identically distributed. Data handling techniques in cases of non-stationary, dependent spatial datasets is still an active area of research.

Once $\delta_{\min}$ is determined, the shape (α) and scale (σ) parameters are estimated using the maximum likelihood method (Grimshaw 1993): 95% confidence intervals for α and σ are asymptotically estimated using normal distributions for α and for log(σ) (Kotz and Nadarajah 2000). Goodness of fit is assessed by means of the A^2 test (Anderson and Darling 1952), a nonparametric test that is especially appropriate for models based on long-tailed distributions (Stephens 1986). Confidence levels for A^2 are obtained by randomly generating, for each model, 5000 data samples from the respective GP distribution characterised by each maximum likelihood estimated pair (α, σ) from the original dataset.

For each vegetation type, POT is applied to the exceedances x of all fire pixels that were recorded during the study period (July–August 2007 to 2009). Obtained models, hereafter referred to as static models, may be improved by incorporating daily anomalies, FWI^*, as a covariate of scale parameter in the GP distributions, in particular by assuming a linear dependence of σ on FWI^*:

$$G(x,\ FWI^*|\alpha, a, b) = 1 - \left(1 + \frac{\alpha}{a \times FWI^* + b} x\right)^{-\frac{1}{\alpha}} \qquad (5)$$

Estimates of shape parameter (α) and of coefficients of the linear relationship $\sigma = a \times FWI^* + b$ are again obtained using the maximum likelihood method. Performance of the new alternative models, hereafter referred to as daily models, is compared against the respective null models (i.e. the original static models) by using the so-called standard likelihood ratio test (Neyman and Pearson 1933). The test is based on statistic Λ defined as:

$$\Lambda = 2(\ln L' - \ln L) \qquad (6)$$

where L is the maximum likelihood function of the static model and L' is the maximum likelihood function of the daily model.

Meteorological danger

Static models allow estimation of baseline danger D_{b0}, which represents the probability that exceedance x is above a given fixed threshold x_0:

$$D_{b0} = D_b(x_0) = 1 - G_{static}(x_0|\alpha, \sigma) \qquad (7)$$

Conversely, the threshold value of exceedance x_0, corresponding to a specified level of baseline danger (D_{b0}) may be estimated, for each vegetation cover type, by inverting the previous relationship:

$$x_0 = x(D_{b0}) = G^{-1}_{static}(1 - D_{b0}) \qquad (8)$$

In a similar way, daily models allow estimation of daily danger (D_d), which represents the probability that exceedance x is above a given fixed threshold x_0 for a given value of FWI^*:

$$D_d(x_0, FWI^*) = 1 - G_{daily}(x_0, FWI^*|\alpha, a, b) \qquad (9)$$

It is worth noting that probabilities as estimated by both static and daily models are conditional on the fact that an event with duration $\delta > \delta_{min}$ has occurred (i.e. all events with duration lower than minimum threshold are excluded). Therefore, baseline and daily dangers (D_b and D_d), which represent probabilities that exceedance x is above a given fixed threshold (x_0), are also conditioned by the occurrence of an event exceeding the minimum threshold.

The role played by meteorological conditions on wildfire potential may then be uncovered by defining meteorological danger (D_m), which combines information about static and daily danger for a given day and pixel according to the following procedure:

1. a given threshold of baseline danger (D_{b0}) is fixed over the entire study area
2. for each vegetation cover, baseline thresholds of exceedances x_0 are computed using the appropriate static models of fire duration (Eqn 8)
3. for each day and pixel location, daily models are then used to estimate daily danger (D_d) based on the corresponding baseline threshold and the observed daily value of FWI^* (Eqn 9)
4. meteorological danger (D_m) is finally defined by the ratio of daily danger (D_d) to prescribed baseline danger (D_{b0}):

$$D_m(x_0, FWI^*) = \frac{D_d(x_0, FWI^*)}{D_{b0}} \qquad (10)$$

Meteorological danger provides a coherent basis to set break points in FWI^* to be used in the definition of classes of meteorological fire danger. Given a baseline danger D_b, break point BP_L will be defined as the value of FWI^* associated to meteorological danger L, that is:

$$D_m(x_0, BP_L) = \frac{D_d(x_0, BP_L)}{D_{b0}} = \frac{1 - G_{daily}(x_0,\ BP_L\,|\alpha, a, b)}{D_{b0}} = L \qquad (11)$$

Values of BP_L may be estimated by inverting the previous equation, for example, using the bisection method (Faires and Burden 1985).

Results

General characteristics of fire duration

The dependence of fire behaviour on vegetation cover may be identified by analysing the spatial distribution of fire duration δ for forest, shrublands and cultivated areas (Table 2). Cultivated areas are the predominant vegetation type, covering 49% of the study area. However, the number of pixels with fire activity of short duration ($\delta \leq 3$ h) only accounts for 28% of the total amount, and steeply decreases with increasing δ, down to 6% for fire duration longer than 9 h. A contrasting behaviour may be observed in the case of shrublands that, despite covering only 20% of the study area, are associated with 29% of the total number of pixels with fire activity of short duration, this amount steeply increasing up to 53% for $\delta > 9$ h. Covering 31% of the study area, forests are associated with the largest fraction (43%) of pixels for $\delta \leq 3$ h; an increase to 48% of pixels is observed for durations in the intervals 3–6 h and 6–9 h, followed by a decrease to 41% for duration larger than 9 h.

Duration of fire activity for the three vegetation types (Table 3) is characterised by long-tailed distributions, with values of $\delta < 3$ h representing ~85, 82 and 94% of the sample in the case of forest, shrubland and cultivated areas. Besides being less frequent in both absolute and relative terms, duration of fire activity in cultivated areas has a shorter tail than duration in forest or shrubland. For instance, the relative frequencies of very long-lasting fire activity ($\delta > 12$ h) over forest and shrubland are 0.52 and 0.89%, about three times and more than five times the value of 0.17% corresponding to cultivated areas. Long-lasting fire episodes are therefore more expected in shrublands and forests than in agricultural areas, a result in close agreement with findings in previous works either at the scale of the Mediterranean basin (Moreira *et al.* 2011; Fernandes 2013) or at the national levels of Portugal (Barros and Pereira 2014), Spain (Moreno *et al.* 2011) and Italy (Bajocco and Ricotta 2008). Such differences in land cover burning are likely to be driven by different interacting factors including fuel connectivity, topography, population density, meteorological conditions and fire suppression (Brotons *et al.* 2013). For instance, the proximity of agricultural lands to populated areas and the social and economic value attributed to agricultural activities is expected to steer an increase of the level of effort in fire suppression and therefore to a decrease in the likelihood of large fire events (Moreira *et al.* 2010, 2011).

Table 2. Dependence of fire duration δ on vegetation type

The first pair of rows presents the distribution of all pixels in study area among the three types of vegetation as derived from GLC2000. The remaining four pairs of rows present the distribution among vegetation types for different ranges of fire duration δ as identified during the study period July–August 2007 to 2009. For each class the absolute frequency is shown together with the relative frequency (%)

Vegetation type	Forest	Shrubland	Cultivated area	Total
Study area	38 076	25 021	61 423	124 520
%	31	20	49	100
$\delta \leq 3$ h	3321	2240	2205	7766
%	43	29	28	100
3 h $< \delta \leq$ 6 h	387	292	118	797
%	48	37	15	100
6 h $< \delta \leq$ 9 h	128	114	23	265
%	48	43	9	100
$\delta > 9$ h	54	71	8	133
%	41	53	6	100

Static models

Results from the previous exploratory analysis suggest choosing POT and GP distributions to model the exceedances of duration δ for each vegetation type. This approach is also in agreement with the results by Amraoui *et al.* (2010) who found that duration of active fires as detected from SEVIRI tends to follow GP distributions over the northern and southern sectors of Africa.

For each vegetation type, a common minimum threshold of 3 h was therefore set for δ_{min} based on the following procedure:

1. Successive thresholds were tested, starting at zero and ending at 6 h with increasing steps of 0.25 h. Values of thresholds were then plotted against the respective sample means exceeding the prescribed thresholds (Coles 2001). The chosen value of 3 h lies in the section of the curve where the excess mean becomes a linear function of thresholds.
2. GP distributions were fitted for successive thresholds, and maximum likelihood estimates of both shape and scale parameters were plotted against the thresholds in order to check for their stability (Castillo and Hadi 1997). The chosen value of 3 h lies in the section of the curve where values of the shape parameter tend to stabilise after a steep decreasing.
3. Degree of fitness of GP distributions was assessed for the successive thresholds using the A^2 test. The confidence levels obtained for the chosen value of 3 h (Table 4) are lower than 95% for shrublands and cultivated areas and lower than 99% for forest, indicating that the null hypothesis that the samples follow a GP distribution cannot be rejected at least at the respective 5 and 1% significance levels.
4. The obtained sample size and respective percentile of the original sample were estimated for the successive thresholds.

Table 4. Static GP models for each vegetation type

Columns 1–5 indicate vegetation type, sample size and corresponding percentile of original data sample (%), estimated values and 95% confidence intervals (in parentheses) of the shape (α) and scale (σ) parameters, and confidence levels (*CL*) of the Anderson–Darling test (Anderson and Darling 1952)

Vegetation type	Sample size (percentile)	α	σ	*CL*
Forest	569 (85%)	−0.06 (−0.13, 0.02)	2.92 (2.61, 3.26)	98%
Shrubland	477 (82%)	−0.14 (−0.22, −0.05)	3.70 (3.27, 4.18)	93%
Cultivated	149 (94%)	−0.01 (−0.15, 0.12)	2.31 (1.87, 2.86)	91%

Table 3. Distribution frequencies of fire activity for the three types of vegetation

The distributions of fire activity refer to the study period of July–August 2007 to 2009; for each class the absolute frequency is shown together with the relative frequency (%)

Classes of duration δ (h)	0.25–3.00	3.25–6.00	6.25–9.00	9.25–12.00	12.25–15.00	15.25–18.00	18.25–21.00	Total
Forest	3321	387	128	34	15	4	1	3890
%	85.37	9.95	3.29	0.87	0.39	0.10	0.03	100.00
Shrubland	2240	292	114	47	17	7	0	2 717
%	82.44	10.75	4.19	1.73	0.63	0.26	0.00	100.00
Cultivated	2205	118	23	4	3	1	0	2 354
%	93.67	5.01	0.98	0.17	0.13	0.04	0.00	100.00

The chosen value of 3 h is associated with sample sizes of 569, 477 and 147 events for forest, shrubland and cultivated areas, representing cuts above percentiles 85, 82 and 94 of the original samples (Table 4).

5. The spatial and temporal distributions of fire events with duration above 3 h were checked to verify whether choice of threshold was high enough to mitigate the effects of temporal and spatial dependence of exceedances. For each vegetation type (Fig. 2), the events with duration $\delta \geq 3$ h were spread throughout the 3-year period; the ones that took place in 2007 (red dots) tending to be more frequent in the eastern Mediterranean, over the Peloponnese and the Balkans in contrast with those that took place in 2009 (blue dots), which are more frequent over the Iberian Peninsula. The year 2008 (green dots) presents a small number of events, especially over Iberia. No temporal structure is apparent in the samples for each vegetation type. The three vegetation types form spatial patches of irregular shape and size, and the observed events with duration $\delta \geq 3$ h are spread over the patches, sometimes concentrating into small clusters of a very few pixels. No spatial structure is apparent in the data; the exception being the large cluster in southern Peloponnese associated with the extreme forest fires that took place from 23–30 August 2007 (San-Miguel-Ayanz *et al.* 2013). This exceptional cluster is nevertheless fragmented among the three classes of vegetation.

The largest scale (σ) parameter is the one for shrubland, followed by forest and cultivated areas (Table 4). The shape (α) parameters are negative for all vegetation cover types,

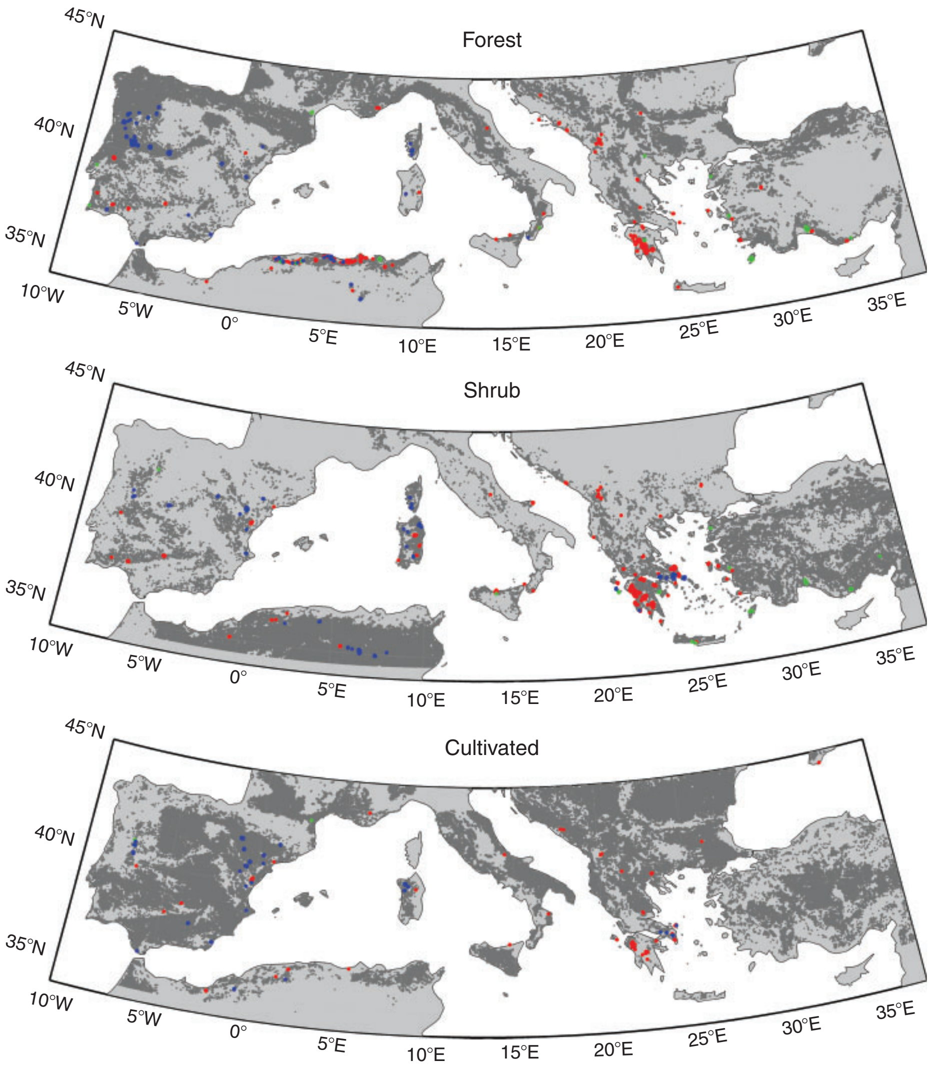

Fig. 2. Geographical distribution of events with fire duration $\delta \geq 3$ h recorded during July–August 2007 to 2009. Each panel is restricted to events in one main vegetation type, namely forests (upper panel), shrublands (middle panel) and cultivated areas (bottom panel). The spatial distribution of each vegetation type is shown in dark grey and the year of occurrence of each event is identified by the colour of the dots (●) for the events of 2007 (red), 2008 (green) and 2009 (blue).

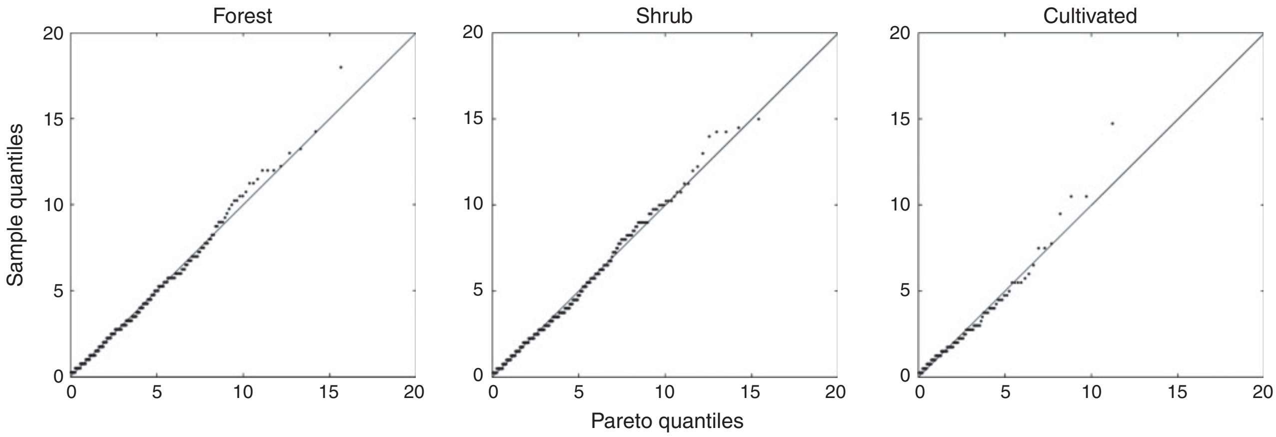

Fig. 3. Probability plots for fitted generalised Pareto models for forest (left panel), shrubland (middle panel) and cultivated area models (right panel). Each plot represents fitted model quantiles (*x*-axis) *v.* sample data quantiles (*y*-axis). Values of quantiles relate to exceedances $x = \delta – \delta_{min}$ (with $\delta_{min} = 3$ h).

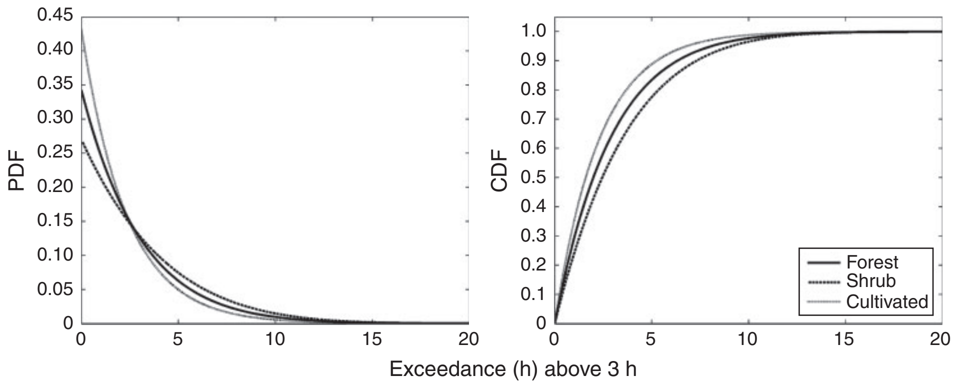

Fig. 4. Probability density functions (left panel) and cumulative distribution functions (right panel) of fitted generalised Pareto models of exceedances $x = \delta - \delta_{min}$ (with $\delta_{min} = 3$ h) for forests (solid curve), shrublands (dashed curve) and cultivated areas (dotted curve).

indicating that exceedances are upper limited. The largest negative value is also the one for shrubland, followed by forest and cultivated areas. The goodness of fit for all vegetation cover types may be visually confirmed by inspecting the probability plots (Fig. 3). The predominant effect of the scale (σ) parameter on the fitted GP models becomes apparent when plotting the cumulative distribution function (CDF) curves for the three vegetation cover types (Fig. 4); the shrubland model presenting the longest tail, followed by forest and cultivated areas.

Daily models

The role played by meteorological factors may be assessed by looking at the effect of FWI on fire activity. The dataset of exceedances *x* for each vegetation type was subdivided into subgroups associated with different ranges of FWI; 51 groups of fire pixels were defined as respectively associated with values of FWI between the 0 and 50th percentiles, between the 1st and 51st percentiles, and so on up to between the 51st and 100th percentiles. GP distributions were then adjusted to each subset and plots were made of estimated values of scale σ *v.* the mean value of FWI in the considered range.

For all types of vegetation cover (Fig. 5), the scale (σ) parameter tends to linearly increase with increasing FWI. Each type presents a characteristic range of FWI, the largest values being observed for shrubland and the lowest for forest. There is a close relationship between vegetation cover and range of FWI, which may be revealed by comparing the geographical distribution of vegetation types (Fig. 1) with that of mean values of FWI during the study period (July–August 2007 to 2009; Fig. 6). However the spatial distribution of FWI is affected by factors other than vegetation. For instance, the eastern and southern borders of the Mediterranean basin present higher values of FWI. The effect of regional factors other than vegetation may be mitigated by replacing daily values of FWI at a given pixel by respective departures (*FWI**) from 30-year means for the reference period 1980–2009.

The effect of meteorological conditions was therefore modelled by introducing *FWI** as a covariate of the scale parameter of the GP models using linear relationships of the type $\sigma = a + b \times FWI^*$ (Table 5). In all cases *P*-values of the maximum likelihood ratio test are lower than 0.5%, meaning that the null hypothesis that the daily models have a better fit than the

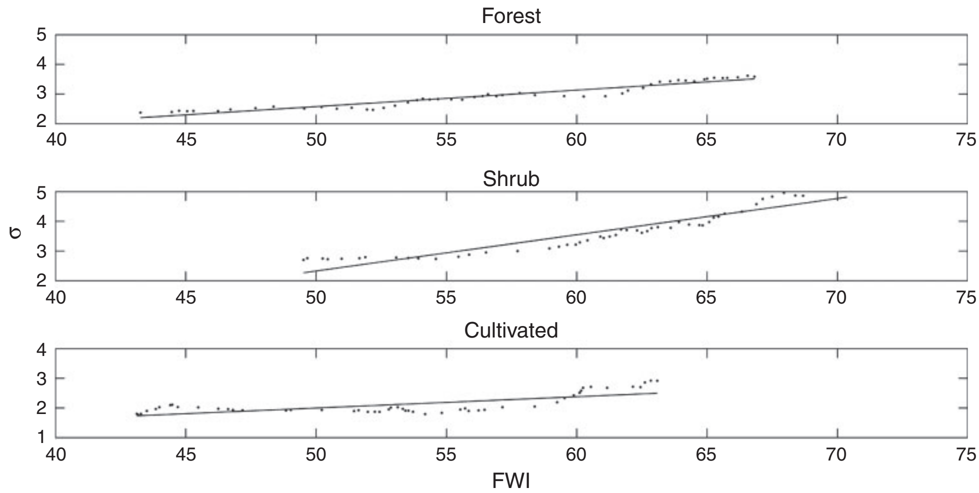

Fig. 5. Dependence on Fire Weather Index of scale parameters of generalised Pareto models for forests (upper panel), shrublands (middle panel) and cultivated areas (lower panel). Straight lines were obtained by linear regression.

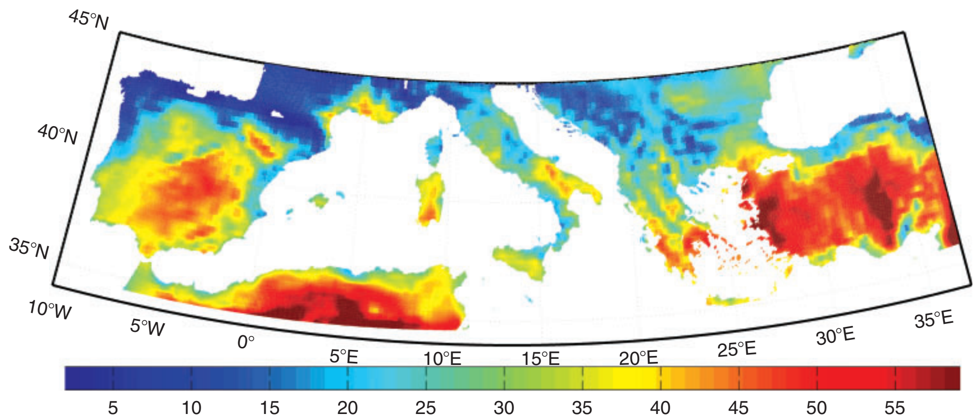

Fig. 6. Geographical distribution of mean values of Fire Weather Index during July–August 2007 to 2009.

Table 5. Daily GP models for each vegetation type

Columns 2–4 indicate the shape (α) parameter, dependence of scale (σ) parameter on *FWI** and *P*-values of the maximum likelihood ratio tests

Vegetation type	α	$\sigma = a + b \times FWI^*$	*P*-value (%)
Forest	−0.074	$\sigma = 2.04 + 0.038 \times FWI^*$	1.39×10^{-5}
Shrub	−0.15	$\sigma = 2.37 + 0.052 \times FWI^*$	1.20×10^{-6}
Cultivated	−0.027	$\sigma = 1.33 + 0.042 \times FWI^*$	0.46

corresponding static ones cannot be rejected at the 0.5% significance level. The sensitivity of scale parameters to changes in *FWI** also reflect on the probabilities of exceedance of duration (Fig. 7).

Calibration of FWI

For each vegetation type the respective static and daily models were used to compute the dependence of meteorological danger D_m on *FWI** (Eqn 10). For a fixed baseline danger $D_b = 33\%$, four break points of *FWI** were obtained, associated to levels of meteorological danger of 0.25, 0.50, 0.75 and 1.00 (Fig. 8). Estimates of break points (Table 6) were obtained by solving Eqn 11 using the bisection method. The three vegetation types present differences that are worth noting. The largest value of the baseline threshold of fire duration (associated with baseline danger $D_b = 33\%$) is the one of shrubland ($x_0 = 3.8$ h) followed at similar intervals of ~0.6–0.7 h by forest ($x_0 = 3.1$ h) and cultivated areas ($x_0 = 2.5$ h). The difference between break points $BP_{1.00}$ and $BP_{0.25}$ is largest for forest (reaching 41.5), followed by shrublands (36.6) and cultivated areas (30.6). Break points for forest are the lowest for all levels of meteorological danger, whereas $BP_{0.50}$ and $BP_{1.00}$ present the highest values for shrubland and $BP_{0.25}$ and $BP_{0.75}$ rank first for cultivated areas, the latter value being closely followed by shrubland.

The four defined break points allow the definition of five classes of meteorological fire danger (Fig. 8): 'low' when $D_m < 0.25$, 'moderate' when $0.25 \le D_m < 0.5$, 'high' when

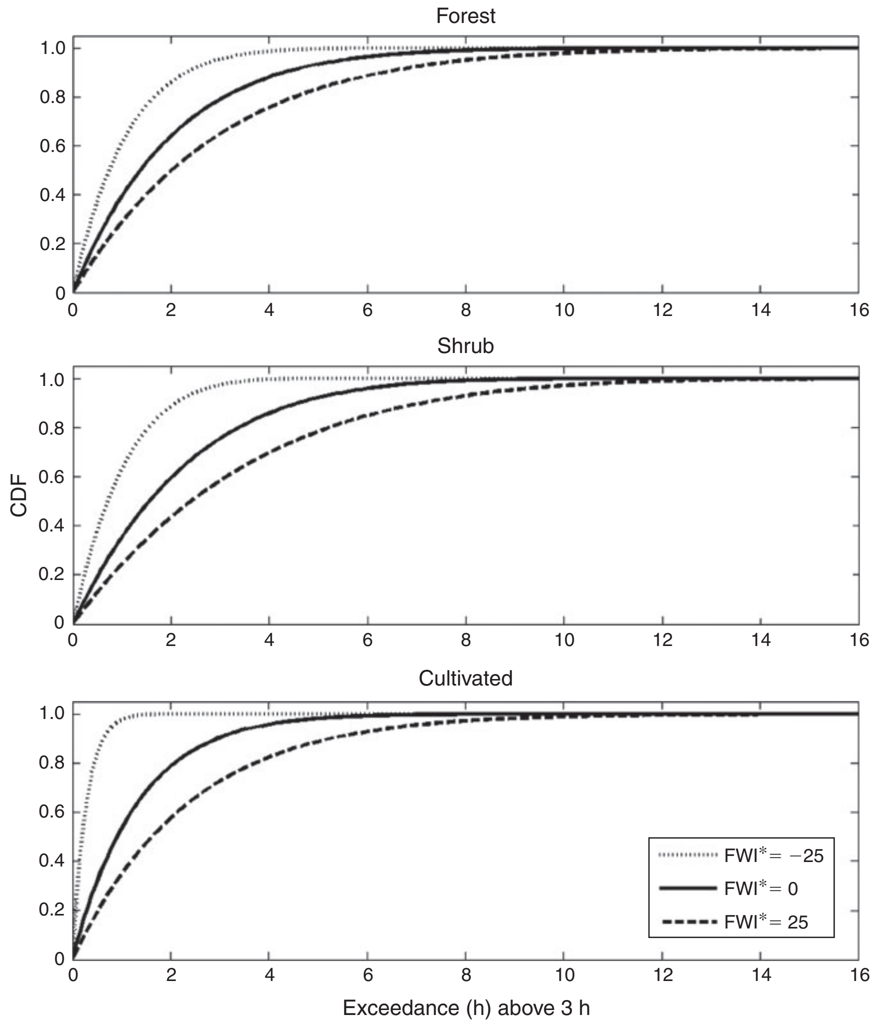

Fig. 7. Cumulative distribution function (CDF) curves for three fixed values of FWI* (−25, 0 and +25) in the case of the daily generalised Pareto model for forests (top panel), shrubs (middle panel) and cultivated areas (bottom panel).

$0.5 \leq D_m < 0.75$, 'very high' when $0.75 \leq D_m < 1$ and 'extremely high' when $D_m \geq 1$.

Discussion

The case of 25 August 2007, when Greece and Albania were struck by very severe fire events, provides an interesting example of the obtained product that is worth analysing in detail. Two impressive clusters of fire pixels with duration >6 h may be observed over Greece (Fig. 9, bottom panel). The larger cluster spreads over the western Peloponnese and contains a large number of fires that lasted >12 h, and the other one locates over eastern Attica and Evia. The map of classes of fire danger (Fig. 9, top panel) shows that both clusters are part of a large core labelled 'extremely high', which covers the entire territory of Greece and extends eastwards into Anatolia and towards the north-east over Bulgaria and Romania up to Crimea. An event lasting >12 h also occurred in Albania, inside a large patch labelled 'very high', which covers the territories of Albania, Montenegro and Bosnia and Herzegovina, and extends towards the north-east up to Ukraine. Several events of short duration (<3 h) also took place within this patch, over Dalmatia, East Thrace and Crimea. Another large patch labelled 'very high' extends over central and southern Italy, which has three events of short duration located along the western coast. A stream of fires of short duration may be identified along the Mediterranean coast of Africa over a region covered by large patches labelled 'very high' and 'extremely high'. The north-western part of the Iberian Peninsula is also covered by a large patch labelled 'very high' with a small nucleus labelled 'extremely high', where an event of short duration took place. No fire events occurred in regions labelled 'low', and 'moderate'. Fire events are virtually absent from the class labelled 'high', the only exception consisting of a fire of short duration that took place in Sicily.

An assessment of the global consistency (in space and time) of results obtained was performed by analysing, for the entire study area and the entire study period, the number of observed events that belong to a given interval of fire duration and were assigned to a given class of fire danger (Table 7). The percentage of fires

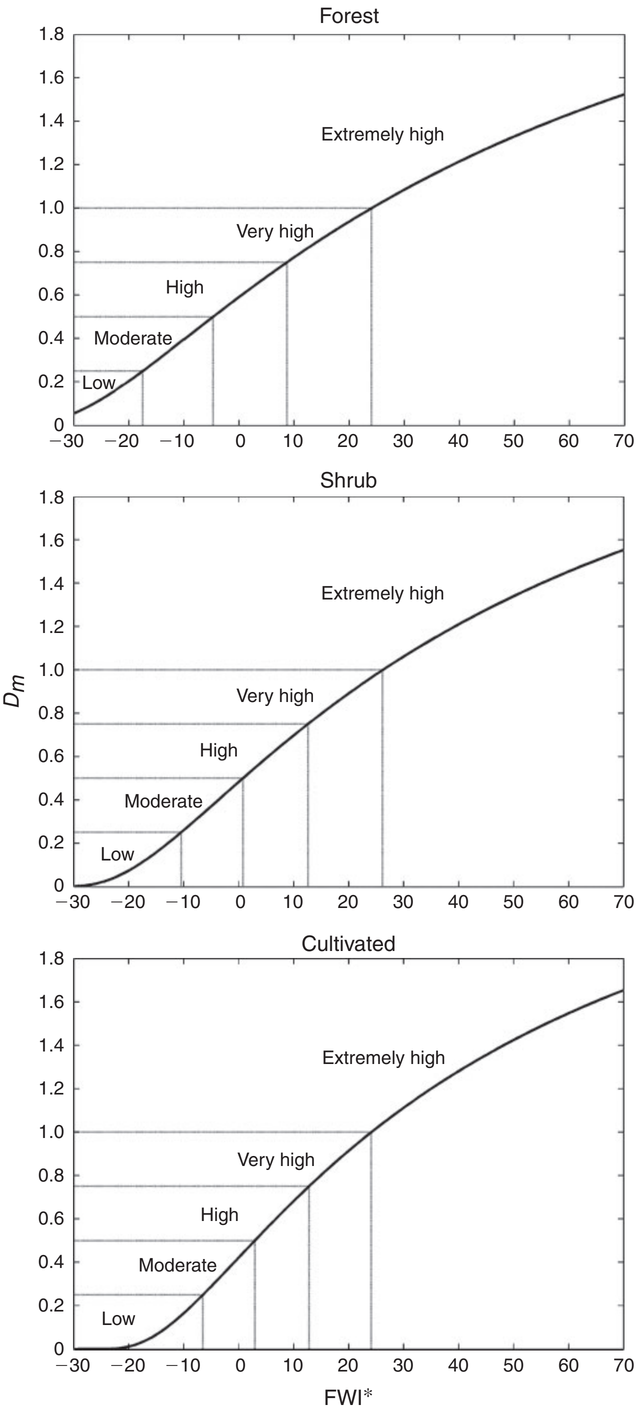

Fig. 8. Dependence of meteorological danger (D_m) on anomalies of Fire Weather Index (*FWI**) and classes of danger for forests (upper panel), shrublands (middle panel) and cultivated areas (lower panel).

within any given duration interval (first numbers in parentheses) steadily decreases with decreasing danger, with the exception of fires of very short duration (<1 h) where the 'high' class is the modal one. Such decrease is especially steep in the cases of the upper intervals of duration. With the exception of fires of very short duration where the fraction is only 1%, there is no fire activity in the case of 'low' danger. When considering fixed classes of danger, it may be noted that the percentage of events associated with any given duration interval (second numbers in parentheses) always decreases with increasing duration; the steepest declines being observed in the lower danger classes.

When looking at maps of classes of fire danger (Fig. 9) it may be noted that areas of 'high' and 'very high' fire danger spread over regions where no fire activity is detected. This is to be expected because both static and daily models allow computing probabilities of exceedance provided there is an event with minimum duration of 3 h. Such conditioning by ignition sources is related to structural risk (Chuvieco and Congalton 1989), which is assessed by means of a set of variables that range from fuel structure and terrain characteristics to human activities and climate variability. Choice of relevant variables and evaluation of structural risk involves studying statistical relationships between long-term records of variables and fire events. Such an endeavour is beyond the scope of this study.

Table 6. Break points of FWI* for each vegetation type

Lines 2–6 indicate baseline threshold of fire duration (x_0) associated with a fixed baseline danger ($D_b = 33\%$) and break points of *FWI** ($BP_{0.25}$, $BP_{0.50}$, $BP_{0.75}$ and $BP_{1.00}$) corresponding to different levels (L) of meteorological danger D_m (0.25, 0.50, 0.75 and 1.00)

	Forest	Shrubland	Cultivated
x_0	3.1 h	3.8 h	2.5 h
$BP_{0.25}$	−17.5	−10.4	−6.5
$BP_{0.50}$	−4.7	0.8	−2.9
$BP_{0.75}$	8.7	12.6	12.8
$BP_{1.00}$	24.0	26.2	24.1

Conclusions

Mediterranean Europe is characterised by cool, wet winters followed by hot, dry summers making the region especially prone to the occurrence of a large number of fires, especially when the summer season is affected by extreme weather events. There are several rating systems of fire danger, but the CFFWIS is one of the most used throughout the world. CFFWIS is particularly adequate to rate fire danger in the Mediterranean, but has to be calibrated in order to take into account specific characteristics of climate and fuel type, fire regime and even the structure of prevention and firefighting.

The calibration approach adopted in this study is based on an integrated use of information about meteorological conditions provided by the ECMWF, vegetation land cover from Global Land Cover 2000 (GLC2000) and fire duration as detected by the SEVIRI instrument on-board MSG satellites. The main difference of the proposed methodology from existing ones is that it takes full advantage of the temporal resolution of SEVIRI, which allows detection of fire events every 15 min. This information is used to make daily records of fire duration that are essential to calibrate meteorological danger and establish classes of fire danger. Traditional approaches rely on calibration procedures performed through analyses of fire weather history based on ground observations of amount of burned area or number of fire occurrences. Several factors may affect the reliability of ground observations; recorded values are not only

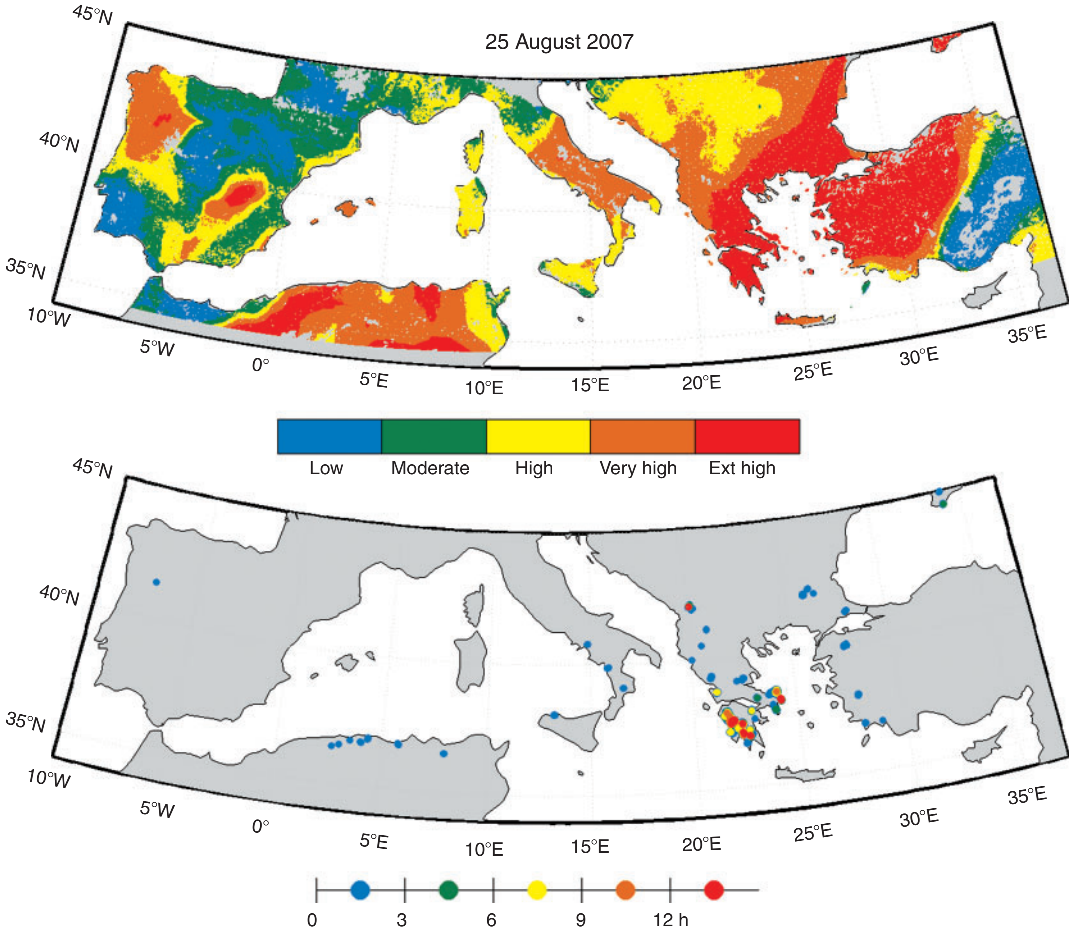

Fig. 9. Map of classes of fire danger (top panel) and corresponding spatial distribution of observed fire events and respective duration (bottom panel) for 25 August 2007. Colours represent classes of fire danger (upper panel) and fire duration (lower panel).

Table 7. Distribution of fire events by classes of fire danger and by fire duration

Each cell contains the number of observed daily fire events and numbers in parentheses are the corresponding fraction (%) of the total number of events with the same fire duration interval followed by the corresponding fraction (%) of the total number of events in the same class of fire danger

Duration (h)	Class of fire danger: Low	Moderate	High	Very high	Extremely high	All classes
0–1	68 (1, 99)	634 (11, 89)	2111 (35, 75)	1853 (31, 66)	1327 (22, 53)	5983 (100, –)
1–2	1 (0, 1)	46 (4, 6)	361 (31, 13)	379 (32, 13)	382 (33, 15)	1169 (100, –)
2–3	0 (0, 0)	14 (3, 2)	132 (22, 5)	215 (37, 8)	225 (38, 9)	586 (100, –)
3–6	0 (0, 0)	12 (2, 2)	180 (23, 6)	267 (33, 9)	338 (42, 14)	797 (100, –)
6–9	0 (0, 0)	7 (3, 1)	29 (11, 1)	77 (29, 3)	150 (57, 6)	263 (100, –)
9–12	0 (0, 0)	0 (0, 0)	6 (7, 0)	28 (33, 1)	51 (60, 2)	85 (100, –)
12–15	0 (0, 0)	0 (0, 0)	2 (6, 0)	8 (23, 0)	25 (71, 1)	35 (100, –)
15–18	0 (0, 0)	0 (0, 0)	1 (8, 0)	3 (25, 0)	8 (67, 0)	12 (100, –)
>18	0 (0, 0)	0 (0, 0)	0 (0, 0)	0 (0, 0)	1 (100, 0)	1 (100, –)
All durations	69 (–, 100)	703 (–, 100)	2822 (–, 100)	2830 (–, 100)	2507 (–, 100)	8931 (100, –)

determined by visual inspection – which may nevertheless affect their accuracy – but also by the policy of individual countries, which may further change in time (Pereira *et al.* 2011). Approaches based on the use of satellite data have the advantage of being more consistent in space and time. They also benefit from not depending on the availability of ground fire records from each country, which are neither easily obtainable, nor available in the short-term.

Finally, it is worth stressing that the FRM product is entirely based on a set of estimated probabilities, in particular meteorological danger. These probabilities are derived from statistical models that may be readily updated and continuously tuned, which represents an advantage from the operational point of view. The fact that the FRM product is currently being disseminated within the framework of the LSA SAF will also allow tailoring of the product according to specific needs of a broad community of users.

Acknowledgements

This study was performed within the framework of the EUMETSAT LSA SAF. Part of the research was supported by the EU 7th Framework Program through project FUME (contract number 243888). The Portuguese Science Foundation (FCT) has supported the research work by M. Amraoui (grant SFRH/BD/36964/2007), S. L. Ermida (grant in project PTDC/AAC-AMB/104702/2008) and K. F. Turkman (projects PEst-OE/MAT/UI0006/2011 and PTDC/MAT/118335/2010).

References

Amraoui M, DaCamara CC, Pereira JMC (2010) Detection and monitoring of African vegetation fires using MSG-SEVIRI imagery. *Remote Sensing of Environment* **114**, 1038–1052. doi:10.1016/J.RSE.2009.12.019

Amraoui M, Liberato MLR, Calado TJ, DaCamara CC, Coelho LP, Trigo RM, Gouveia CM (2013) Fire activity over Mediterranean Europe based on information from Meteosat-8. *Forest Ecology and Management* **294**, 62–75. doi:10.1016/J.FORECO.2012.08.032

Anderson TW, Darling DA (1952) Asymptotic theory of certain 'goodness of fit' criteria based on stochastic processes. *Annals of Mathematical Statistics* **23**, 193–212. doi:10.1214/AOMS/1177729437

Andrews PL, Loftsgaarden DO, Bradshaw LS (2003) Evaluation of fire danger indexes using logistic regression and percentile analysis. *International Journal of Wildland Fire* **12**, 213–226. doi:10.1071/WF02059

Bajocco S, Ricotta C (2008) Evidence of selective burning in Sardinia (Italy): which land-cover classes do wildfires prefer? *Landscape Ecology* **23**, 241–248. doi:10.1007/S10980-007-9176-5

Barros AMG, Pereira JMC (2014) Wildfire selectivity for land cover type: does size matter? *PLoS ONE* **9**, e84760. doi:10.1371/JOURNAL.PONE.0084760

Bartholomé E, Belward AS (2005) GLC2000: a new approach to global land cover mapping from Earth Observation data. *International Journal of Remote Sensing* **26**, 1959–1977. doi:10.1080/01431160412331291297

Bovio G, Camia A (1997) Meteorological indices for large fires danger rating. In 'A Review of Remote Sensing Methods for the Study of Large Wildland Fires'. Megafires project ENV-CT96–0256 (Ed. E Chuvieco) pp. 73–90. (Universidad de Alcalá: Alcalá de Henares, Spain)

Brotons L, Aquilué N, de Cáceres M, Fortin M-J, Fall A (2013) How fire history, fire suppression practices and climate change affect wildfire regimes in Mediterranean landscapes. *PLoS ONE* **8**, e62392. doi:10.1371/JOURNAL.PONE.0062392

Camia A, Amatulli G (2009) Weather factors and fire danger in the Mediterranean. In 'Earth Observation of Wildland Fires in Mediterranean Ecosystems'. (Ed. E Chuvieco) pp. 71–82. (Springer-Verlag: Berlin)

Carvalho A, Flannigan M, Logan K, Miranda A, Borrego C (2008) Fire activity in Portugal and its relationship to weather and the Canadian Fire Weather Index System. *International Journal of Wildland Fire* **17**, 328–338. doi:10.1071/WF07014

Castillo E, Hadi AS (1997) Fitting the generalized Pareto distribution to data. *Journal of the American Statistical Association* **92**, 1609–1620. doi:10.1080/01621459.1997.10473683

Chuvieco E, Congalton RG (1989) Application of remote sensing and geographic information systems to forest fire hazard mapping. *Remote Sensing of Environment* **29**, 147–159. doi:10.1016/0034-4257(89)90023-0

Chuvieco E, González I, Verdú F, Aguado I, Yebra M (2009) Prediction of fire occurrence from live fuel moisture content measurements in a Mediterranean ecosystem. *International Journal of Wildland Fire* **18**, 430–441. doi:10.1071/WF08020

Chuvieco E, Aguado I, Yebra M, Nieto H, Salas J, Martín MP, Vilar L, Martínez J, Martín S, Ibarra P, de la Riva J, Baeza J, Rodríguez F, Molina JR, Herrera MA, Zamora R (2010) Development of a framework for fire risk assessment using remote sensing and geographic information system technologies. *Ecological Modelling* **221**, 46–58. doi:10.1016/J.ECOLMODEL.2008.11.017

Coles S (2001) 'An Introduction to Statistical Modeling of Extreme Values.' (Springer-Verlag: London)

de Zea Bermudez P, Kotz S (2010*a*) Parameter estimation of the generalized Pareto distribution – Part I. *Journal of Statistical Planning and Inference* **140**, 1353–1373. doi:10.1016/J.JSPI.2008.11.019

de Zea Bermudez P, Kotz S (2010*b*) Parameter estimation of the generalized Pareto distribution – Part II. *Journal of Statistical Planning and Inference* **140**, 1374–1388. doi:10.1016/J.JSPI.2008.11.020

de Zea Bermudez P, Mendes J, Pereira JMC, Turkman KF, Vasconcelos MJP (2009) Spatial and temporal extremes of wildfire sizes in Portugal (1984–2004). *International Journal of Wildland Fire* **18**, 983–991. doi:10.1071/WF07044

Dimitrakopoulos AP, Mitsopoulos ID, Gatoulas K (2010) Assessing ignition probability and moisture of extinction in a Mediterranean grass fuel. *International Journal of Wildland Fire* **19**, 29–34. doi:10.1071/WF08124

Dimitrakopoulos AP, Bemmerzouk AM, Mitsopoulos ID (2011) Evaluation of the Canadian fire weather index system in an eastern Mediterranean environment. *Meteorological Applications* **18**, 83–93. doi:10.1002/MET.214

Embrechts P, Kluppelberg C, Mikosch T (1997) 'Modelling Extremal Events: For Insurance and Finance.' (Springer: Berlin).

EUMETSAT (1999) LRIT/HRIT global specification. EUMETSAT, Coordination group for meteorological satellites, CGMS 03. (Darmstadt, Germany)

EUMETSAT (2010) MSG level 1.5 image data format description. EUMETSAT, EUM/MSG/ICD/105. (Darmstadt, Germany)

European Commission (2008) Forest Fires in Europe 2007, EUR 23492 EN, Office for Official Publications of the European Communities. (Luxembourg)

European Commission (2009) Forest Fires in Europe 2008, EUR 23971 EN, Office for Official Publications of the European Communities. (Luxembourg)

European Commission (2010) Forest Fires in Europe 2009, EUR 24502 EN, Publication Office of the European Union. (Luxembourg)

European Commission (2011) Forest Fires in Europe 2010, EUR 24910 EN, Publication Office of the European Union. (Luxembourg)

Faires JD, Burden RL (1985) 'Numerical Analysis.' (Prindle, Weber & Schmidt: Boston, MA)

Fernandes PM (2008) Forest fires in Galicia (Spain): the outcome of unbalanced fire management. *Journal of Forest Economics* **14**, 155–157. doi:10.1016/J.JFE.2007.11.002

Fernandes PM (2013) Fire-smart management of forest landscapes in the Mediterranean basin under global change. *Landscape and Urban Planning* **110**, 175–182. doi:10.1016/J.LANDURBPLAN.2012.10.014

Finney MA (2005) The challenge of quantitative risk analysis for wildland fire. *Forest Ecology and Management* **211**, 97–108. doi:10.1016/J.FORECO.2005.02.010

Fujioka FM, Gill AM, Viegas DX, Wotton BM (2008) Fire danger and fire behavior modeling systems in Australia, Europe and North America. *Developments in Environmental Science* **8**, 471–497. doi:10.1016/S1474-8177(08)00021-1

Grimshaw SD (1993) Computing maximum likelihood estimates for the generalized Pareto distribution. *Technometrics* **35**, 185–191. doi:10.1080/00401706.1993.10485040

Holmes TP, Huggett RJ Jr, Westerling AL (2008) Statistical analysis of large wildfires. In 'The Economics of Forest Disturbances: Wildfires, Storms, and Invasive Species'. (Eds TP Holmes, JP Prestemon JP, KL Abt) Vol. 79, pp. 59–77. (Springer Forestry Sciences Series: Berlin)

Kiil AD, Miyagawa RS, Quintilio D (1977) Calibration and performance of the Canadian fire weather index in Alberta. Canadian Forestry Service, Northern Forest Research Centre, Information Report NOR-X-173. (Edmonton, AB)

Kotz S, Nadarajah S (2000) 'Extreme Value Distributions: Theory and Applications.' (Imperial College Press: London)

Lavorel S, Flannigan MD, Lambin EF, Scholes MC (2007) Vulnerability of land systems to fire: interactions between humans, climate, the atmosphere and ecosystems. *Mitigation and Adaptation Strategies for Global Change* **12**, 33–53. doi:10.1007/S11027-006-9046-5

Lawrence MG (2005) The relationship between relative humidity and the dewpoint temperature in moist air: a simple conversion and applications. *Bulletin of the American Meteorological Society* **86**, 225–233. doi:10.1175/BAMS-86-2-225

Lloret F, Calvo E, Pons X, Díaz-Delgado R (2002) Wildfires and landscape patterns in the Eastern Iberian Peninsula. *Landscape Ecology* **17**, 745–759. doi:10.1023/A:1022966930861

Mataix-Solera J, Cerdà A, Arcenegui VA, Jordán A, Zavala LM (2011) Fire effects on soil aggregation: a review. *Earth-Science Reviews* **109**, 44–60. doi:10.1016/J.EARSCIREV.2011.08.002

Mendes JM, de Zea Bermudez PC, Pereira J, Turkman KF, Vasconcelos MJP (2010) Spatial extremes of wildfire sizes: Bayesian hierarchical models for extremes. *Environmental and Ecological Statistics* **17**, 1–28. doi:10.1007/S10651-008-0099-3

Moreira F, Catry FX, Rego F, Bacao F (2010) Size-dependent pattern of wildfire ignitions in Portugal: when do ignitions turn into big fires? *Landscape Ecology* **25**, 1405–1417. doi:10.1007/S10980-010-9491-0

Moreira F, Viedma O, Arianoutsou M, Curt T, Koutsias N, Rigolot E, Barbati A, Corona P, Vaz P, Xanthopoulos G, Mouillot F, Bilgili E (2011) Landscape–wildfire interactions in Southern Europe: implications for landscape management. *Journal of Environmental Management* **92**, 2389–2402. doi:10.1016/J.JENVMAN.2011.06.028

Moreno JM, Vázquez A, Vélez R (1998) Recent history of forest fires in Spain. In 'Large Forest Fires'. (Ed. JM Moreno) pp. 159–185. (Backhuys Publishers: Leiden)

Moreno JM, Viedma O, Zavala G, Luna B (2011) Landscape variables influencing forest fires in central Spain. *International Journal of Wildland Fire* **20**, 678–689. doi:10.1071/WF10005

Neyman J, Pearson ES (1933) On the problem of the most efficient tests of statistical hypotheses. Philosophical Transactions of the Royal Society of London – A. Mathematical and Physical Sciences 231, 289–337.

Pausas JG, Vallejo R (1999) The role of fire in European Mediterranean ecosystems. In 'Remote Sensing of Large Wildfires in the European Mediterranean Basin'. (Ed. E Chuvieco) pp. 3–16. (Springer-Verlag: Berlin)

Pereira MG, Trigo RM, DaCamara CC, Pereira JMC, Leite SM (2005) Synoptic patterns associated with large summer forest fires in Portugal. *Agricultural and Forest Meteorology* **129**, 11–25. doi:10.1016/J.AGRFORMET.2004.12.007

Pereira MG, Malamud BD, Trigo RM, Alves PI (2011) The history and characteristics of the 1980–2005 Portuguese rural fire database. *Natural Hazards and Earth System Sciences* **11**, 3343–3358. doi:10.5194/NHESS-11-3343-2011

Pereira MG, Calado TJ, DaCamara CC, Calheiros T (2013) Effects of regional climate change on rural fires in Portugal. *Climatic Change* **57**, 187–200.

Pickands J, III (1975) Statistical inference using extreme order statistics. *Annals of Statistics* **3**, 119–131. doi:10.1214/AOS/1176343003

San-Miguel-Ayanz J, Carlson JD, Alexander M, Tolhurst K, Morgan G, Sneeuwjagt R, Dudley M (2003) Current methods to assess fire danger potential. In 'Wildland Fire Danger Estimation and Mapping'. (Ed. E Chuvieco) pp. 20–61. (World Scientific Publishing: Singapore)

San-Miguel-Ayanz J, Schulte E, Schmuck G, Camia A, Strobl P, Liberta G, Giovando C, Boca R, Sedano F, Kempeneers P, McInerney D, Withmore C, Santos de Oliveira S, Rodrigues M, Durrant T, Corti P, Oehler F, Vilar L, Amatulli G (2012) Comprehensive monitoring of wildfires in Europe: the European Forest Fire Information System (EFFIS). In 'Approaches to Managing Disaster – Assessing Hazards, Emergencies and Disaster Impacts'. (Ed. J Tiefenbacher) pp. 87–108. (InTech: Rijeka, Croatia)

San-Miguel-Ayanz J, Moreno JM, Camia A (2013) Analysis of large fires in European Mediterranean landscapes: lessons learned and perspectives. *Forest Ecology and Management* **294**, 11–22. doi:10.1016/J.FORECO.2012.10.050

Stephens MA (1986) Tests based on EDF statistics. In 'Goodness-of-Fit Techniques'. (Eds RB D'Agostino, MA Stephens) pp. 97–193. (Marcel Dekker: New York)

Stocks BJ, Lawson BD, Alexander ME, Van Wagner CE, McAlpine RS, Lynham TJ, Dube DE (1989) The Canadian Forest Fire Danger Rating System: an overview. *Forestry Chronicle* **65**, 450–457. doi:10.5558/TFC65450-6

Šturm T, Fernandes PM, Šumrada R (2012) The Canadian Fire Weather Index System and wildfire activity in the Karst forest management area, Slovenia. *European Journal of Forest Research* **131**, 829–834. doi:10.1007/S10342-011-0556-7

Sun C, Tolver A (2012) Assessing the distribution patterns of wildfire sizes in Mississippi, USA. *International Journal of Wildland Fire* **21**, 510–520. doi:10.1071/WF10107

Trigo RM, Pereira JM, Pereira MG, Mota B, Calado MT, DaCamara CC, Santo FE (2006) Atmospheric conditions associated with the exceptional fire season of 2003 in Portugal. *International Journal of Climatology* **26**, 1741–1757. doi:10.1002/JOC.1333

Trigo IF, DaCamara CC, Viterbo P, Roujean J-L, Olesen F, Barroso C, Camacho-de-Coca F, Carrer D, Freitas SC, García-Haro J, Geiger B, Gellens-Meulenberghs F, Ghilain N, Meliá J, Pessanha L, Siljamo N, Arboleda A (2011) The satellite application facility for land surface analysis. *International Journal of Remote Sensing* **32**, 2725–2744. doi:10.1080/01431161003743199

Van Wagner CE (1974) Structure of the Canadian Forest Fire Weather Index. Canadian Forestry Service, Publication 1333. (Ottawa, ON)

Van Wagner CE (1987) Development and structure of the Canadian Forest Fire Weather Index System. Canadian Forestry Service, Technical Report 35. (Ottawa, ON)

Viegas DX, Viegas MTSP, Ferreira AD (1992) Moisture content of fine forest fuels and fire occurrence in central Portugal. *International Journal of Wildland Fire* **2**, 69–86. doi:10.1071/WF9920069

Viegas DX, Bovio G, Ferreira A, Nosenzo A, Sol B (1999) Comparative study of various methods of fire danger evaluation in southern Europe. *International Journal of Wildland Fire* **9**, 235–246. doi:10.1071/WF00015

Viegas DX, Reis RM, Cruz MG, Viegas MT (2004) Calibration of Canadian Fire Danger Rating System for application to Portugal. *Silva Lusitana* **12**, 77–93.